Energy Levels of Ho^{3+} Ions in Yttrium Gallium Garnet and Yttrium Iron Garnet, and Exchange between Ho^{3+} and Fe^{3+} Ions in Yttrium Iron Garnet

H. KAMIMURA*
Bell Telephone Laboratories, Murray Hill, New Jersey 07974

AND

T. YAMAGUCHI
Department of Physics, University of Tokyo, Tokyo, Japan

(Received 17 November 1969)

Energy levels of a Ho^{3+} ion in YGaG are firstly calculated within the framework of the crystal-field theory. Observed structures of the ground $^5I_8$ and the excited $^5I_7$ manifolds are fairly well reproduced by the three-parameter fit. Then the energy levels of a Ho^{3+} ion in YIG are calculated as functions of the direction of the net magnetization, taking into account the orbitally anisotropic exchange as well as the isotropic one. Comparison between the calculated and observed results on the variation of the energy levels reveals that the orbitally anisotropic exchange plays an important role in the Ho-Fe exchange interaction, and further that the Ho-Fe exchange interaction takes place primarily through the next-nearest-neighbor oxygen ions.

I. INTRODUCTION

THE absorption and emission spectra of Ho^{3+} ions in ferrimagnetic yttrium iron garnet (YIG) and its diamagnetic counterpart yttrium gallium garnet (YGaG) have been reported in an earlier paper,[1] and the present paper is devoted to the analysis of these spectra. The ground term of a Ho^{3+} ion with $(4f)^{10}$ electron configuration is ^5I, which under the influence of spin-orbit interaction breaks up into five manifolds ^5I_J, where $J=4, 5, 6, 7, 8$. Among these manifolds, the state $^5I_8$ has the lowest energy. The absorption and emission spectra reported in the preceding paper correspond to transitions between the lowest manifold $^5I_8$ and the first-excited one $^5I_7$. Thus, in the present paper, particular attention is paid to how the $^5I_8$ and $^5I_7$ manifolds are affected by the crystal field in the case of Ho^{3+} in YGaG and by the combined crystal and exchange fields in the case of Ho^{3+} in YIG.

Several analyses of the crystal-field splitting of *manifolds* in some other rare-earth ions in YAG and YGaG have already been carried out[2–5] and the effect of the exchange field on energy levels has also been investigated for the ground manifold of Tb^{3+} in YIG[6] and for the excited and ground manifolds of Yb^{3+} in YbIG.[7,8] Therefore, our analysis will follow the previous pattern for the most part. Three important conclusions emerge from the present work. The first is that observed structures of the ground $^5I_8$ and the excited $^5I_7$ manifolds of Ho^{3+} ions in YGaG are fairly well reproduced by the three-parameter theory. The second that the strength of electric-quadrupole transitions is smaller by order of 10^5 than that of the magnetic dipole transition, so that electric-quadrupole transitions are not responsible for the observed transitions of Ho^{3+} in YGaG, the intensities of which are of order of the magnetic dipole strength. The third is that the orbitally anisotropic exchange plays an important role in the exchange between Ho^{3+} and Fe^{3+} ions in YIG, in addition to the usual isotropic Heisenberg exchange.

In Sec. II the crystal-field splittings of $^5I_8$ and $^5I_7$ of a Ho^{3+} ion in YGaG are calculated. In Sec. III the crystal-field parameters are determined so as to fit the optical spectra. Then, using the eigenfunctions of the crystal-field states we calculate the f values of magnetic dipole and electric quadrupole transitions. In Sec. IV the energy levels of a Ho^{3+} ion in YIG are calculated as functions of the direction of the magnetization of the iron sublattice by diagonalizing the crystal-field and exchange Hamiltonians simultaneously. Comparison between the calculated and observed variations of spectra as functions of the direction of the magnetization in a $(1\bar{1}0)$ plane indicate that consideration of the orbitally anisotropic exchange terms is necessary, in addition to the ordinary isotropic Heisenberg exchange.

II. CRYSTAL-FIELD CALCULATION FOR $^5I_8$ AND $^5I_7$ MANIFOLDS

According to crystallographic data on YIG and YGaG, yttrium ions which are replaced by rare-earth ions occupy the dodecahedral sites which have D_2 point symmetry. There are six types of dodecahedral site in YIG and YGaG, each having the same orthorhombic symmetry when referred to a system of local axes, which

* Present address: Department of Physics, University of Tokyo, Tokyo, Japan.

[1] L. F. Johnson, J. F. Dillon, Jr., and J. P. Remeika, Phys. Rev. (to be published).

[2] J. A. Koningstein and J. E. Geusic, Phys. Rev. **136**, A711 (1964).

[3] J. A. Koningstein, Phys. Rev. **136**, A717 (1964); J. A. Koningstein and J. E. Geusic, *ibid.* **136**, A726 (1964); M. T. Hutchings and W. P. Wolf, J. Chem. Phys. **41**, 617 (1964).

[4] R. A. Buchanan, K. A. Wickersheim, J. J. Pearson, and G. E. Herrmann, Phys. Rev. **159**, 245 (1967).

[5] J. J. Pearson, G. F. Herrmann, K. A. Wickersheim, and R. A. Buchanan, Phys. Rev. **159**, 251 (1967).

[6] J. F. Dillon, Jr., and L. R. Walker, Phys. Rev. **124**, 1401 (1961).

[7] K. A. Wickersheim and R. L. White, Phys. Rev. Letters **4**, 123 (1960); K. A. Wickersheim, Phys. Rev. **122**, 1376 (1961); K. A. Wickersheim and R. L. White, Phys. Rev. Letters **8**, 483 (1962).

[8] P. M. Levy, Phys. Rev. **135**, A155 (1964); **147**, 311 (1966).

TABLE I. Operator equivalent factors for $^5I_8$ and $^5I_7$.

	$^5I_8$	$^5I_7$
α	$-1/2\times3^2\times5^2$	$1/2\times3\times5\times13$
β	$-1/2\times3\times5\times7\times11\times13$	$1/2\times3^2\times11^2\times13$
γ	$-5/3^3\times7\times11^2\times13^2$	$5/11^2\times13^2\times21\times27$

differ, however, in the spatial orientation of these axes. Thus the crystal-field Hamiltonian for a Ho^{3+} ion which occupies any one of these sites is given by

$$\begin{aligned}V_c=&A_2^0\sum(3z^2-r^2)+A_2^2\sum(x^2-y^2)\\&+A_3^2\sum xyz+A_4^0\sum(35z^4-30r^2z^2+3r^4)\\&+A_4^2\sum(x^2-y^2)(6z^2-x^2-y^2)+A_4^4\sum(x^4-6x^2y^2-y^4)\\&+A_5^2\sum(3z^2-r^2)xyz+A_5^4\sum(x^2-y^2)xyz\\&+A_6^0\sum(231z^6-315r^2z^4+105r^4z^2-5r^6)\\&+A_6^2\sum(x^2-y^2)(16z^4-16x^2z^2-16y^2z^2+x^4+2x^2y^2+y^4)\\&+A_6^4\sum(x^4-6x^2y^2+y^4)(10z^2-x^2-y^2)\\&+A_6^6\sum(x^6-15x^4y^2+15x^2y^4-y^6)\\&+A_7^2\sum(143z^4-110z^2r^2+15r^4)xyz\\&+A_7^4\sum(x^2-y^2)(13z^2-3r^2)xyz\\&+A_7^6\sum(6x^4-20x^2y^2+6y^4)xyz,\quad(1)\end{aligned}$$

where x, y, and z are referred to the local symmetry axes, and the summations run over the ten $4f$ electrons of the holmium ion. The terms of the third, fifth, and seventh orders of the spherical harmonics represent the noncentrosymmetrical field by which a state of the opposite parity is mixed.

In what follows we calculate the effects of V_c on two manifolds $^5I_8$ and $^5I_7$ of Ho^{3+} ions. Since the crystal-field splittings of the levels are of the order of several hundred wave numbers whereas the spacing between

TABLE II. Crystal-field eigenfunctions.

(a) Cyrstal-field eigenfunctions in $^5I_8$

A_1:	$(1/\sqrt2)(\|8,8\rangle+\|8,-8\rangle)$,	$(1/\sqrt2)(\|8,6\rangle+\|8,-6\rangle$,
	$(1/\sqrt2)(\|8,4\rangle+\|8,-4\rangle)$,	$(1/\sqrt2)(\|8,2\rangle+\|8,-2\rangle)$, $\|8,0\rangle$
A_2:	$(1/\sqrt2)(\|8,8\rangle-\|8,-8\rangle)$,	$(1/\sqrt2)(\|8.6\rangle-\|8,-6\rangle)$,
	$(1/\sqrt2)(\|8,4\rangle-\|8,-4\rangle)$,	$(1/\sqrt2)(\|8,2\rangle-\|8,-2\rangle)$
B_1:	$(1/\sqrt2)(\|8,7\rangle-\|8,-7\rangle)$,	$(1/\sqrt2)(\|8,5\rangle-\|8,-5\rangle)$,
	$(1/\sqrt2)(\|8,3\rangle-\|8,-3\rangle)$,	$(1/\sqrt2)(\|8,1\rangle-\|8,-1\rangle)$
B_2:	$(1/\sqrt2)(\|8,7\rangle+\|8,-7\rangle)$,	$(1/\sqrt2)(\|8,5\rangle+\|8,-5\rangle)$,
	$(1/\sqrt2)(\|8,3\rangle+\|8,-3\rangle)$,	$(1/\sqrt2)(\|8,1\rangle+\|8,-1\rangle)$

(b) Crystal-field eigenfunctions in $^5I_7$

A_1:	$(1/\sqrt2)(\|7,6\rangle-\|7,-6\rangle)$,	$(1/\sqrt2)(\|7,4\rangle-\|7,-4\rangle)$,
	$(1/\sqrt2)(\|7,2\rangle-\|7,-2\rangle)$	
A_2:	$(1/\sqrt2)(\|7,6\rangle+\|7,-6\rangle)$,	$(1/\sqrt2)(\|7,4\rangle+\|7,-4\rangle)$,
	$(1/\sqrt2)(\|7,2\rangle+\|7,-2\rangle)$, $\|7,0\rangle$	
B_1:	$(1/\sqrt2)(\|7,7\rangle+\|7,-7\rangle)$,	$(1/\sqrt2)(\|7,5\rangle+\|7,-5\rangle)$,
	$(1/\sqrt2)(\|7,3\rangle+\|7,-3\rangle)$,	$(1/\sqrt2)(\|7,1\rangle+\|7,-1\rangle)$
B_2:	$(1/\sqrt2)(\|7,7\rangle-\|7,-7\rangle)$,	$(1/\sqrt2)(\|7,5\rangle-\|7,-5\rangle)$,
	$(1/\sqrt2)(\|7,3\rangle-\|7,-3\rangle)$,	$(1/\sqrt2)(\|7,1\rangle-\|7,-1\rangle)$

TABLE III. The best set of the crystal-field parameters. Units of cm^{-1}.

$$\begin{aligned}&B_2^0=A_2^0\bar r^2=119\\&B_2^2=A_2^2\bar r^2=161\\&B_4^0=A_4^0\bar r^4=-174\\&B_4^2=A_4^2\bar r^4=5\\&B_4^4=A_4^4\bar r^4=611\\&B_6^0=A_6^0\bar r^6=18\\&B_6^2=A_6^2\bar r^6=-3\\&B_6^4=A_6^4\bar r^6=110\\&B_6^6=A_6^6\bar r^6=-24\end{aligned}$$

$^5I_8$ and $^5I_7$ is 5000 cm^{-1}, it is reasonable to neglect the off-diagonal matrix elements of the crystal-field Hamiltonian (1) between the manifolds and consider the effect of V_c as a perturbation of each manifold. Furthermore, we neglect the terms of the noncentrosymmetrical field in (1) for the calculation of the energy levels. According to our point-charge calculation, the biggest term in the noncentrosymmetrical field A_3^2 is an order of magnitude smaller than the smallest one in the centrosymmetrical part of V_c. Thus the present approximation of neglecting the noncentrosymmetrical part seems reasonable. The effects of the noncentrosymmetrical part are taken into account when we discuss the intensity of optical transitions later, because the electric-dipole transitions between $^5I_8$ and $^5I_7$ become allowed by the presence of the noncentrosymmetrical part.

Under the above approximations and with the use of the operator equivalent method of Stevens,[9] Elliott,[10] and Judd,[11] V_c can be written in the following form for a manifold specified by the quantum numbers $LSJJ_z$.

$$\begin{aligned}V_c=&B_2^0\alpha[3J_z^2-J(J+1)]+B_2^2\alpha\tfrac12(J_+^2+J_-^2)\\&+B_4^0\beta\{35J_z^4-[30J(J+1)-25]J_z^2-6J(J+1)\\&+3J^2(J+1)^2\}+B_4^2\beta\tfrac14\{[7J_z^2-J(J+1)-5]\\&\times(J_+^2+J_-^2)+(J_+^2+J_-^2)[7J_z^2-J(J+1)-5]\}\\&+B_4^4\beta\tfrac12(J_+^4+J_-^4)+B_6^0\gamma\{231J_z^6\\&-105[3J(J+1)-7]J_z^4+[105J^2(J+1)^2\\&-525J(J+1)+294]J_z^2-5J^3(J+1)^3+40J^2(J+1)^2\\&-60J(J+1)\}+B_6^2\gamma\tfrac14\{(33J_z^4-[18J(J+1)+123]J_z^2\\&+J^2(J+1)^2+10J(J+1)+102)(J_+^2+J_-^2)\\&+(J_+^2+J_-^2)(33J_z^4-[18J(J+1)+123]J_z^2\\&+J^2(J+1)^2+10J(J+1)+102)\}+B_6^4\gamma\tfrac14\{11J_z^2\\&-J(J+1)-38\}(J_+^4+J_-^4)+(J_+^4+J_-^4)\\&\times[11J_z^2-J(J+1)-38]\}+B_6^6\gamma\tfrac12(J_+^6+J_-^6),\quad(2)\end{aligned}$$

where α, β, and γ are the operator equivalent factors, and $J_\pm=J_x\pm iJ_y$. The coefficients B_n^m are the crystal-field parameters defined by $B_n^m=A_n^m\bar r^n$, where $\bar r^n=\int[R(r)]^2r^nr^2dr$, $R(r)$ being the radial-part wave function of a single $4f$ electron.

[9] K. W. H. Stevens, Proc. Phys. Soc. (London) **65**, 209 (1952).
[10] R. J. Elliot and K. W. H. Stevens, Proc. Roy. Soc. (London) **218**, 437 (1953); **219**, 553 (1953).
[11] B. R. Judd, Proc. Roy. Soc. (London) **227**, 552 (1955).

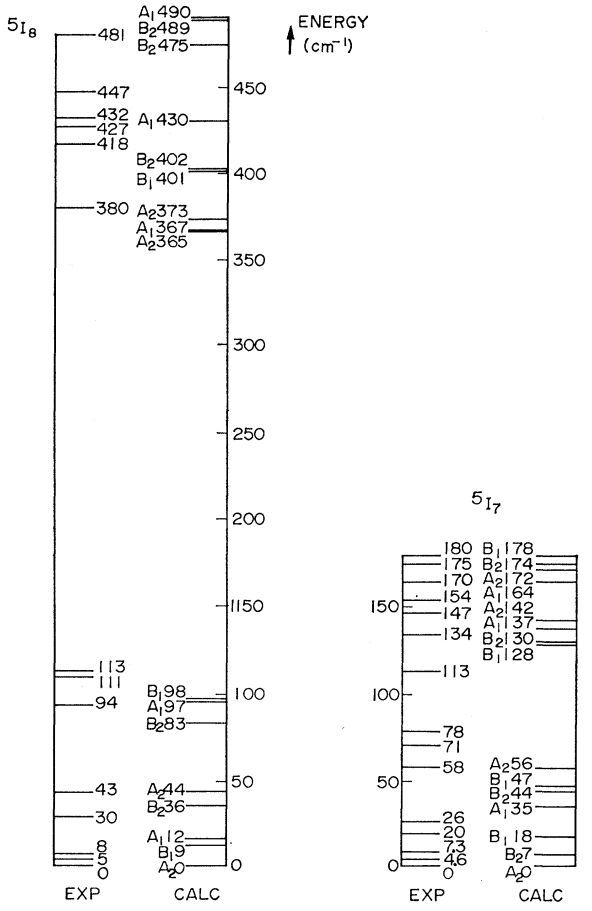

FIG. 1. Energy-level structures of the ground and excited manifolds $^5I_8$, $^5I_7$ of Ho^{3+} ions in YGaG.

Values of α, β, and γ for the $^5I_8$ and $^5I_7$ manifolds of a Ho^{3+} ion are given in Table I. Since the crystal-field Hamiltonian (2) contains nine constants, it is not possible to attempt to vary all of these parameters to fit the optical data. Therefore, following Dillon and Walker,[6] we assume that the point-charge approximation correctly gives the relative sizes of the constants within each order of the spherical harmonics; in other words, the ratios $B_2^0:B_2^2(=A_2^0:A_2^2)$, $B_4^0:B_4^2:B_4^4(=A_4^0:A_4^2:A_4^4)$, and $B_6^0:B_6^2:B_6^4:B_6^6(=A_6^0:A_6^2:A_6^4:A_6^6)$ are taken to be those calculated by them. Thus the number of adjustable crystal-field parameters is reduced to three which we call λ_2, λ_4, and λ_6. The parameters λ_2, λ_4, and λ_6 contain $\bar{r}^2$, $\bar{r}^4$, and $\bar{r}^6$, respectively.

In Sec. III we diagonalize the 17×17 and 15×15 secular equations of V_c for the manifolds $^5I_8$ and $^5I_7$, respectively, and determine λ_2, λ_4, and λ_6 which best fit the observed absorption and emission data of Ho^{3+} ions in YGaG by the least-squares method.

III. ANALYSIS OF SPECTRA OF Ho^{3+} IN YGaG

There are 17 energy levels for the $^5I_8$ ground manifold and 15 energy levels for the $^5I_7$ excited manifold. These energy levels are all one-dimensional and labeled by the irreducible representation of D_2. The $^5I_8$ state splits into five A_1, four A_2, four B_1, and four B_2 by V_c, and the $^5I_7$ state splits into three A_1, four A_2, four B_1, and four B_2.

The four irreducible representations of D_2, A_1, A_2, B_1, and B_2, can be spanned by any linear combination of the corresponding kets (defined by values of J and J_z) set out in Tables II(a) and II(b).

The values of λ_2, λ_4, and λ_6 which give the best account of the experimental results are $\lambda_2=0.4$, $\lambda_4=1.7$, and $\lambda_6=11.0$. These lead to the set of crystal-field parameters shown in Table III. The energy levels for the $^5I_8$ and $^5I_7$ manifolds which are calculated using the crystal-field parameters in Table III are shown in Fig. 1, where the observed values are also shown for the sake of comparison. The discrepancy between theory and experiment is probably due to our approximation in which the relative sizes of the parameters within each order of the spherical harmonics have been fixed to be those of the point-charge approximation. It should be noted from Fig. 1 that the lowest crystal-field states of the $^5I_8$ and $^5I_7$ manifolds are both A_2. This result is not sensitive to the values of parameters λ_2, λ_4, and λ_6 as long as the sign of B_2^0 is positive; in other words, this conclusion holds for a wide range of values for these parameters in the case of positive B_2^0. On the other hand, in the case of a negative B_2^0 the lowest state of $^5I_7$ becomes B_1 although that of $^5I_8$ is still A_2. In this case, however, we have not been able to find any set of λ_2, λ_4, and λ_6 which reproduces the observed absorption and emission spectra fairly well.

In order to examine further whether the parameters obtained are reasonable, we calculate the intensities of all the absorption peaks and compare these with the observed ones. On the basis of the energy diagram, shown in Fig. 1, the character of the optical transitions

TABLE IV. Selection rules.

(a) Selection rules for electric-dipole transitions caused by noncentrosymmetrical field and magnetic-dipole transitions

Initial state	Final state $\mathbf{E}\|x$ $\mathbf{H}\|x$	$\mathbf{E}\|y$ $\mathbf{H}\|y$	$\mathbf{E}\|z$ $\mathbf{H}\|z$
A_1	B_2	B_1	A_2
A_2	B_1	B_2	A_1
B_1	A_2	A_1	B_2
B_2	A_1	A_2	B_1

(b) Selection rule for electric-quadrupole transition [$A_{xx}=\partial A_x/\partial x$, $A_{xy}=(\partial A_x/\partial y+\partial A_y/\partial x)$, etc. $\mathbf{A}$ is the vector potential of the form $\mathbf{A}=A_0\boldsymbol{\pi}e^{i\mathbf{k}\cdot\mathbf{r}}$.]

Initial state	$\frac{1}{3}A_{zz}-\frac{1}{6}A_{xx}$ $-\frac{1}{6}A_{yy}$	$\frac{1}{2}(A_{xx}-A_{yy})$	A_{xy}	A_{yz}	A_{zz}
A_1	A_1	A_1	A_2	B_2	B_1
A_2	A_2	A_2	A_1	B_1	B_2
B_1	B_1	B_1	B_2	A_2	A_1
B_2	B_2	B_2	B_1	A_1	A_2

$^5I_8 \leftrightarrows {}^5I_7$ as well as the selection rules are determined. According to Van Vleck[12] there exist three mechanisms which cause zero-phonon optical transitions between states with the same $(4f)^n$-electron configuration. Namely, (1) electric-dipole transitions caused by noncentrosymmetrical fields, (2) magnetic-dipole transitions, and (3) electric-quadrupole transitions. Since a Ho^{3+} ion in YGaG and YIG occupies a site with D_2 symmetry, all three mechanisms are possible. Selection rules for electric- and magnetic-dipole transitions are given in Table IV(a) while those for electric-quadrupole transitions are given in Table IV(b).

Using the obtained eigenfunctions of the crystal-field states, we calculate the oscillator strengths for the magnetic-dipole and electric-quadrupole transitions from the lowest state of the $^5I_8$ manifold to each state of the $^5I_7$ manifold. Concerning the electric-dipole transitions due to the noncentrosymmetrical field, we determine these from experimental results, because there is no available information on the magnitude of the noncentrosymmetrical field.

The oscillator strength for the magnetic-dipole transition from an initial state i to a final state f is given by

$$f_{\mathrm{mag}}=\frac{4\pi\nu m}{3he^2}|\langle i|\frac{e}{2mc}(\mathbf{L}+2\mathbf{S})|f\rangle|^2 \qquad (3)$$

for unpolarized light, where $\mathbf{L}$ and $\mathbf{S}$ are the orbital and spin angular momentum operators, respectively, and ν is the frequency of the transition under consideration. On the other hand, the oscillator strength for the electric-quadrupole transition in the case of unpolarized light is given by

$$f_{\mathrm{eq}}=\frac{\pi m\nu^3}{10hc^2}\sum_{kl}|\langle i|Q_{kl}|f\rangle|^2, \qquad (4)$$

where Q_{kl} is the quadrupole tensor $r_k r_l - r^2\delta_{kl}$ ($r_1=x$, $r_2=y$, $r_3=z$).

Since the initial state i is the lowest state of the ground manifold A_2, the final state f in the magnetic-dipole transitions is A_1, B_1, or B_2 while that in the electric-quadrupole transitions is A_2 according to Tables IV(a) and IV(b). The calculated values of f_{mag} and f_{eq} are tabulated in Table V, where the observed values are also shown for the sake of comparison. It is seen from this table that the calculated values of f_{eq} are always too small to explain the observed f values of the corresponding transitions between A_2 states. Thus we can conclude that the transitions between the states of the same symmetry in Ho^{3+} ions in garnets are not due to the electric-quadrupole one. The observed intensities of these transitions may be explained by mixing of A_2 states with states of other symmetry induced by, for example, the existence of impurity ions or imperfections

[12] J. H. Van Vleck, J. Phys. Chem. 41, 67 (1937); J. Chem. Phys. 7, 72 (1939).

TABLE V. The oscillator strengths of all absorption peaks from the A_2 ground state of $^5I_8$.

Frequency (cm^{-1})	Assignment $^5I_8 \rightarrow {}^5I_7$	$10^8 f$ (observed)	f value $10^{13} f_{\mathrm{eq}}$	$10^8 f_{\mathrm{mag}}$
5210.8	$A_2 \rightarrow A_2$	2.6	2.6	
5214.8	$\rightarrow B_2$	···		0.003
5218.1	$\rightarrow B_1$	2.1		0.33
5230.9	$\rightarrow A_1$	2.3		1.5
5237.2	$\rightarrow B_2$	0.3		0.24
5268.7	$\rightarrow B_1$	2.6		1.6
5282.3	$\rightarrow A_2$	1.5	6.1	
5289	$\rightarrow B_1$	0.3		0.24
5324	$\rightarrow B_2$	<0.07		2.1
5345.3	$\rightarrow A_1$	1.3		0.002
5358.2	$\rightarrow A_2$	9.8	3.2	
5364.8	$\rightarrow A_1$	3.6		5.14
5380.6	$\rightarrow A_2$	···	45.0	
5385.9	$\rightarrow B_2$	6.4		6.5
5391.4	$\rightarrow B_1$	1.4		2.0

near Ho^{3+} ions. Since energy levels of Ho^{3+} ions in the ground and excited manifolds appear closely as seen in Fig. 1, such mixing is expected to be large.

Concerning the transitions between states of different symmetry, the calculated values of f_{mag} are of the same order of magnitude as the observed f values for most of the transitions. We can ascribe the discrepancy between the calculated f_{mag} and the observed ones to the contribution from electric-dipole transitions caused by the noncentrosymmetrical field which we have neglected for the calculation of the energy levels. This is because electric-dipole transitions are also possible to the states for which the magnetic-dipole transitions are allowed and their f values, f_{el}, are estimated to be of the order of 10^{-8} by $f_{\mathrm{el}} \sim f_{\mathrm{allowed}} \times (V_{\mathrm{odd}}/\Delta E)^2$, where the magnitude of the noncentrosymmetrical part, V_{odd}, has been assumed to be 1 cm^{-1} from the results of the point-charge calculation and ΔE has been taken to be the energy difference between $^5I_8$ and $^5I_7$ ($\sim 5.2\times 10^3$ cm^{-1}). Only for the peaks at 5324 and 5345.3 cm^{-1} is the discrepancy between the calculated f_{mag} and the observed one too large to be attributed to the contribution from electric-dipole transitions. This might be due to our approximation of three parameters.

IV. ENERGY LEVELS OF A Ho^{3+} ION IN YIG

Now we are in a position to calculate the energy levels of a Ho^{3+} ion in YIG. Since there exists an exchange interaction between the magnetic moment of the Ho ion and that of the iron sublattice in the case of YIG, we must take this into account in writing the Hamiltonian for the Ho^{3+} ion in YIG.

In YIG the iron ions form two nonidentical sublattices which we call A and D sublattices. A Ho ion interacts magnetically with the Fe^{3+} ions on the A and D sublattices. We first assume that the exchange interaction between the Ho ion and the Fe^{3+} ions on A and D sublattices is expressed as the isotropic Heisenberg

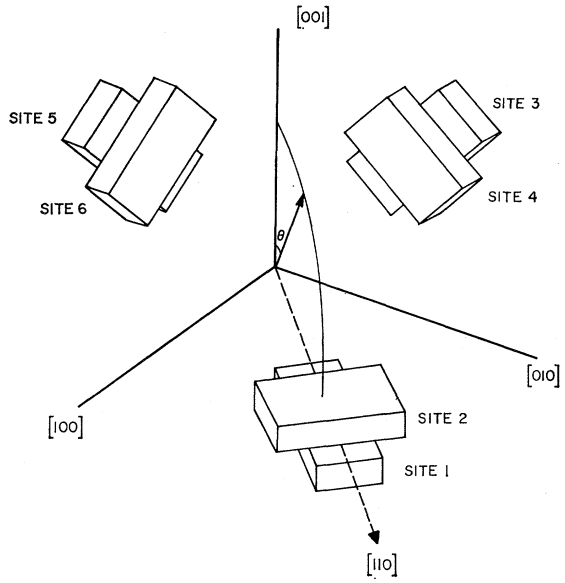

FIG. 2. Relative orientation of the six inequivalent types of dodecahedral site in YIG (after Ref. 6).

Hamiltonian

$$H_{\rm ex}{}^{(1)}=\sum_a J_{ac}\mathbf{S}_c\cdot\mathbf{S}_a+\sum_d J_{cd}\mathbf{S}_c\cdot\mathbf{S}_d\,, \tag{5}$$

where $\mathbf{S}_c$, $\mathbf{S}_a$, and $\mathbf{S}_{\rm d}$ are the spins of the Ho ion, the Fe^{3+} ions on A and D sublattices, respectively.

As we see below, however, the detailed analysis of the optical spectra of Ho-doped YIG will reveal that agreement with experiment cannot be obtained by the above exchange Hamiltonian. As was pointed out by Van Vleck[13] and Levy,[8] the exchange interaction between the S-state paramagnetic ion Fe^{3+} and the f electrons of a rare-earth ion can in general be expressed by orbitally anisotropic terms in addition to the isotropic term because of the directional dependence of orbital charge density of the f electrons. In fact, the importance of the anisotropic exchange has recently been stressed by many authors.[7,14–17] Therefore, in order to interpret the observed spectra we take into account the orbitally anisotropic exchange interaction, in addition to the above isotropic exchange term (5).

In the present problem, orbital anisotropy in the exchange interaction between Ho^{3+} and Fe^{3+} ions arises from the directional dependence of the charge densities of the f electrons of a Ho^{3+} ion. Thus the exchange interaction between a Ho^{3+} ion and its neighboring Fe^{3+} ions at a and d sites can be written as

$$H_{\rm ex}=\sum_a\sum_{k=0}^{6}\sum_{q=-k}^{k}\sum_{i=1}^{10}\alpha_{kq}{}^{a}T_q{}^{[k]}(i)\mathbf{s}_i\cdot\mathbf{S}_a +\sum_d\sum_{k=0}^{6}\sum_{q=-k}^{k}\sum_{i=1}^{10}\beta_{kq}{}^{d}T_q{}^{[k]}(i)\mathbf{s}_i\cdot\mathbf{S}_d\,, \tag{6}$$

where i refers to the f electrons of Ho^{3+} and $T_q{}^{[k]}(i)$ is the qth component of the kth irreducible tensorial operator which acts on the orbital part of the rare-earth wave function. Further time-reversal symmetry restricts k in (6) to even integers.

Using the fact that the A and D iron sublattices are ferrimagnetically coupled, namely,

$$-\mathbf{S}_a=\mathbf{S}_{\rm d}\equiv\mathbf{S}_{\rm Fe}\,, \tag{7}$$

and with the use of the operator equivalent method, $H_{\rm ex}$ of (6) can be replaced by the following expression for a manifold specified by $LSJJ_z$:

$$\begin{aligned}H_{\rm ex}=\{&a_{00}+a_{20}[3J_z{}^2-J(J+1)]+a_{22}\tfrac{1}{2}(J_+{}^2+J_-{}^2)\\&+a_{40}(35J_z{}^4-[30J(J+1)-25]J_z{}^2-6J(J+1)\\&+3J^2(J+1)^2)+a_{42}\tfrac{1}{4}([7J_z{}^2-J(J+1)-5]\\&\times(J_+{}^2+J_-{}^2)+(J_+{}^2+J_-{}^2)[7J_z{}^2-J(J+1)-5])\\&+a_{44}\tfrac{1}{2}(J_+{}^4+J_-{}^4)+a_{60}(231J_z{}^6-105[3J(J+1)-7]\\&\times J_z{}^4+[105J^2(J+1)^2-525J(J+1)+294]J_z{}^2\\&-5J^3(J+1)^3+40J^2(J+1)^2-60J(J+1))\\&+a_{62}\tfrac{1}{4}[(33J_z{}^4-[18J(J+1)+123]J_z{}^2+J^2(J+1)^2\\&+10J(J+1)+102)(J_+{}^2+J_-{}^2)+(J_+{}^2+J_-{}^2)\\&\times(33J_z{}^4-[18J(J+1)+123]J_z{}^2+J^2(J+1)^2\\&+10J(J+1)+102)]+a_{64}\tfrac{1}{4}([11J_z{}^2-J(J+1)\\&-38](J_+{}^4+J_-{}^4)+(J_+{}^4+J_-{}^4)[11J_z{}^2-J(J+1)\\&-38])+a_{66}\tfrac{1}{2}(J_+{}^6+J_-{}^6)\}\mathbf{S}_c\cdot\mathbf{S}_{\rm Fe}\\\equiv&A_{op}(\mathbf{J})\mathbf{S}_c\cdot\mathbf{S}_{\rm Fe}\,,\end{aligned} \tag{8}$$

where we have assumed that a Ho site has D_2 symmetry.

Since the exchange interaction between the Fe^{3+} ions on A and D sublattices is strong compared with J_{ac} and J_{cd} defined in (5), we may consider that the magnetization of the iron sublattices is almost saturated at 4 and 20°K at which measurements have been made. Therefore, we may replace $\mathbf{S}_{\rm Fe}$ by $\mathbf{M}_0/gN\beta$, where $\mathbf{M}_0$ is the net saturation magnetization of the iron sublattices, β is the Bohr magneton, g is the g value of a Fe^{3+} ion, and N is the number of Fe^{3+} ions in the crystal.

Let us apply an external magnetic field so as to vary the direction of $\mathbf{M}_0$. In this case the direction of $\mathbf{M}_0$ is that of the applied magnetic field (the easy axis of $\mathbf{M}_0$ is the [111] direction). Since $\mathbf{S}_c$ is proportional to the total angular momentum operator $\mathbf{J}$ within the manifold with $J=$const, the exchange Hamiltonian (8) can be rewritten as follows:

$$H_{\rm ex}=cA_{op}(\mathbf{J})(\mathbf{N}_i\cdot\mathbf{J})\,, \tag{9}$$

where $\mathbf{N}_i$ is a unit vector in the direction of the applied

[13] J. H. Van Vleck, Phys. Rev. **52**, 1178 (1937); Rev. Mat. Fís. Téor., Tucumán, Argentina **14**, 189 (1962).
[14] M. T. Hutchings, C. G. Windsor, and W. P. Wolf, Phys. Rev. **148**, 444 (1966).
[15] M. Tachiki and Z. Sroubek, Solid State Commun. **5**, 361 (1967).
[16] N. L. Huang and J. H. Van Vleck, Solid State Commun. **6**, 557 (1968).
[17] N. L. Huang and J. H. Van Vleck, J. Appl. Phys. **40**, 1144 (1969).

field and c is given by

$$c=|\mathbf{M}_0||\mathbf{S}_c|/gN\beta|\mathbf{J}|. \quad (10)$$

We choose the components of the magnetic field with regard to the orthorhombic axes of each site in which the crystal-field Hamiltonian is simplified as in (2). Therefore, the N_i differ from site to site.

The complete Hamiltonian for the Ho^{3+} ion in YIG is now expressed by the sum of (2) and (9), that is,

$$H=V_c+H_{ex}. \quad (11)$$

The matrix elements of the Hamiltonian (11) within the manifolds with $J=8$ and 7 are easily calculated for each of the six sites in the $LSJJ_z$ scheme. The energy levels of the ground ($J=8$) and excited ($J=7$) manifolds are found by diagonalizing the 17×17 and 15×15 secular equations, respectively. We consider the case in which the direction of the magnetic field is varied in the $(1\bar{1}0)$ plane. In this case the N_i are given by

$$N_1=[0, \sin\theta, \cos\theta], \quad (12a)$$

$$N_2=[-\sin\theta, 0, \cos\theta], \quad (12b)$$

$$N_3=[-(\cos\theta/\sqrt{2})(1-\tan\theta/\sqrt{2}), (\cos\theta/\sqrt{2})(1+\tan\theta/\sqrt{2}), \sin\theta/\sqrt{2}], \quad (12c)$$

$$N_4=[-(\cos\theta/\sqrt{2})(1+\tan\theta/\sqrt{2}), -(\cos\theta/\sqrt{2})(1-\tan\theta/\sqrt{2}), \sin\theta/\sqrt{2}], \quad (12d)$$

$$N_5=[(\cos\theta/\sqrt{2})(1+\tan\theta/\sqrt{2}), -(\cos\theta/\sqrt{2})(1-\tan\theta/\sqrt{2}), \sin\theta/\sqrt{2}], \quad (12e)$$

$$N_6=[(\cos\theta/\sqrt{2})(1-\tan\theta/\sqrt{2}), (\cos\theta/\sqrt{2})(1+\tan\theta/\sqrt{2}), \sin\theta/\sqrt{2}], \quad (12f)$$

where θ is measured from the [001] axis.

As seen in Fig. 2, the number of inequivalent sites in this case is four. Sites 3 and 5, and also sites 4 and 6 become equivalent. Each energy level is calculated as a function of the direction of the magnetization θ. In doing so, however, we must know the values of λ_2, λ_4, λ_6 and ten exchange parameters $\tilde{a}_{kq}$, where $\tilde{a}_{kq}=ca_{kq}$. Since the spectra of Ho in YIG are complicated because of the existence of the exchange field, it is not easy to determine λ_2, λ_4, λ_6, and $\tilde{a}_{kq}$'s from the spectra of Ho in YIG. Therefore, we use the crystal-field parameters λ_2, λ_4, and λ_6 obtained for Ho^{3+} in diamagnetic YGaG in the calculation of the energy levels of Ho^{3+} in YIG. Then, fitting the variation of the calculated energy levels as functions of θ to the observed data, we determine the ten exchange parameters $\tilde{a}_{kq}$. Since the lattice constants of YIG and YGaG are nearly the same, it is reasonable to use the crystal-field parameters of Ho in YGaG in the case of Ho in YIG.

First, we put $\tilde{a}_{kq}=0$ except the isotropic component $\tilde{a}_{00}$, that is, we consider only the isotropic exchange interaction whose original expression is given in (5). In this case if we choose $\tilde{a}_{00}=2.0$ cm^{-1}, the observed splittings of the lower crystal-field states in $^5I_8$ due to

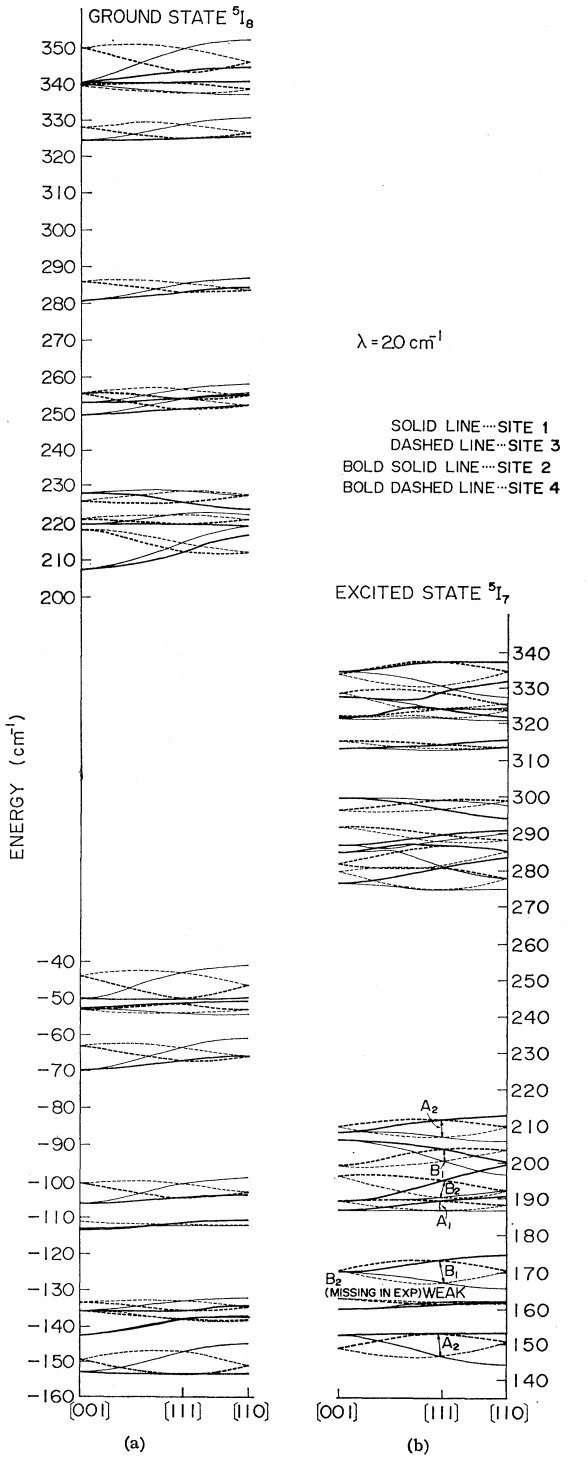

FIG. 3. (a) Energy levels of $^5I_8$ for the four inequivalent sites in YIG as functions of the angle θ in the $(1\bar{1}0)$ plane between the (001) axis and the direction of the net magnetization, in the case of the isotropic exchange, $\tilde{a}_{00}=2$ cm^{-1} and other $\tilde{a}_{kq}=0$. (b) Energy levels of $^5I_7$ as functions of θ in the case of $\tilde{a}_{00}=2$ cm^{-1} and other $\tilde{a}_{kq}=0$.

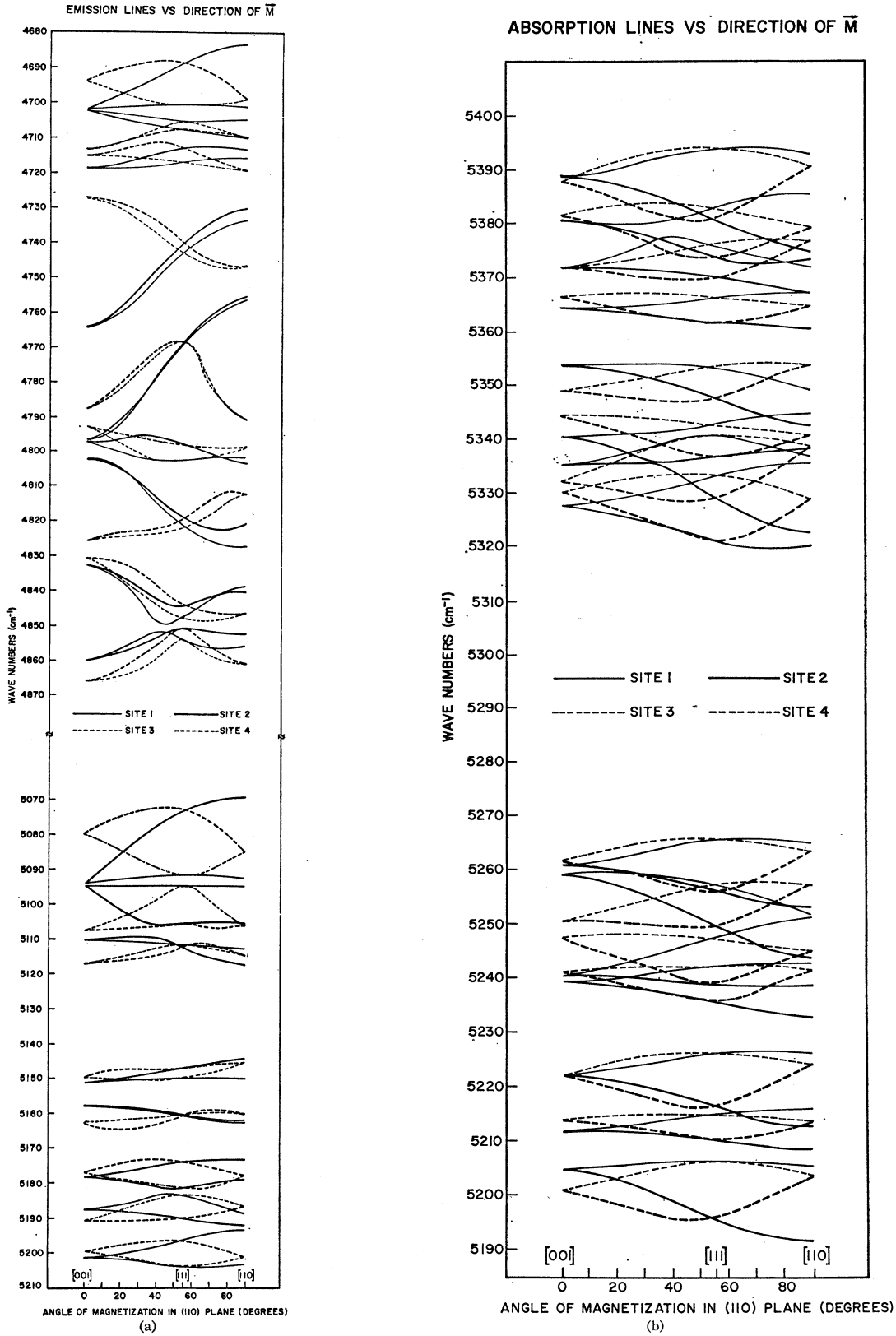

FIG. 4. (a) Energy levels of ${}^5I_8$ as functions of θ in the presence of the orbitally anisotropic as well as the isotropic exchange terms with the values of $\tilde{a}_{kq}$'s shown in Table VI. (b) Energy levels of ${}^5I_7$ as functions of θ for the anisotropic exchange parameters in Table VI.

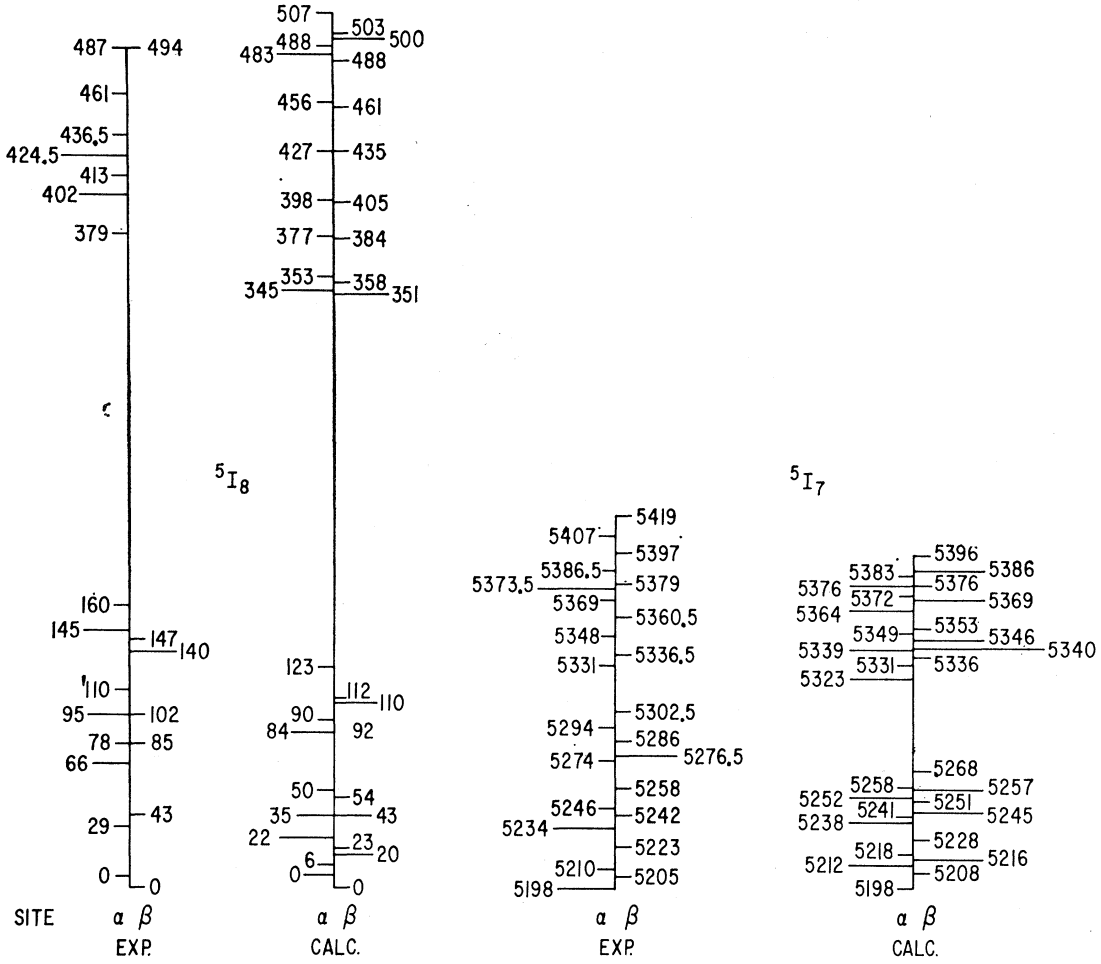

FIG. 5. Energy levels of $^5I_8$ and $^5I_7$ of Ho^{3+} in YIG with the net magnetization directing along the [111] direction (no external magnetic field). There are two sets of the inequivalent sites which we call α for sites 1, 3, and 5, and β for sites 2, 4, and 6. In this figure, the exchange-field splittings of the lowest states of manifolds excited and ground states of manifolds are assumed to be 7 cm^{-1} and zero, respectively, where the sum of these splittings is known experimentally to be 7 cm^{-1} (see Ref. 1).

the exchange field are reproduced fairly well. Figures 3(a) and 3(b) represent the energy levels of $^5I_8$ and $^5I_7$, respectively, for the four inequivalent sites in YIG as functions of θ in the $(1\bar{1}0)$ plane in the case of $\tilde{a}_{00}$ $=2.0$ cm^{-1}. It is seen from these figures and the observed variation shown in Figs. 6 and 7 of Ref. 1 that the variation of the group of the lower energy levels with the direction of the magnetization coincides with the observed one fairly well while that of the higher energy levels is significantly different from the observed one. For a group of the higher energy levels the variation of each calculated energy level with θ is small compared with the observed one. In order to reproduce the large variation of higher energy levels, we must choose a larger value of $\tilde{a}_{00}$. For a larger value of $\tilde{a}_{00}$, however, the agreement between the calculated and observed variation becomes worse for the group of lower energy levels.

Thus the above results suggest that the ordinary isotropic exchange interaction is not sufficient to reproduce the observed variation of all the energy levels of the ground and excited manifolds. Therefore we must proceed to take into account the effects of orbitally anisotropic exchange terms. Thus now we solve (11) with (8) and (2) which includes the ten exchange parameters. These ten exchange parameters $\tilde{a}_{kq}$'s are determined so as to reproduce the observed variation of optical spectra as functions of θ fairly well. The values of $\tilde{a}_{kq}$'s thus

TABLE VI. The best set of the exchange parameters (cm^{-1}).

$\tilde{a}_{00}=2.5$
$\tilde{a}_{20}=-0.04$
$\tilde{a}_{22}=-0.11$
$\tilde{a}_{40}=-8$
$\tilde{a}_{42}=-4.5$
$\tilde{a}_{44}=84$
$\tilde{a}_{60}=0.06$
$\tilde{a}_{62}=-0.02$
$\tilde{a}_{64}=-0.07$
$\tilde{a}_{66}=-0.24$

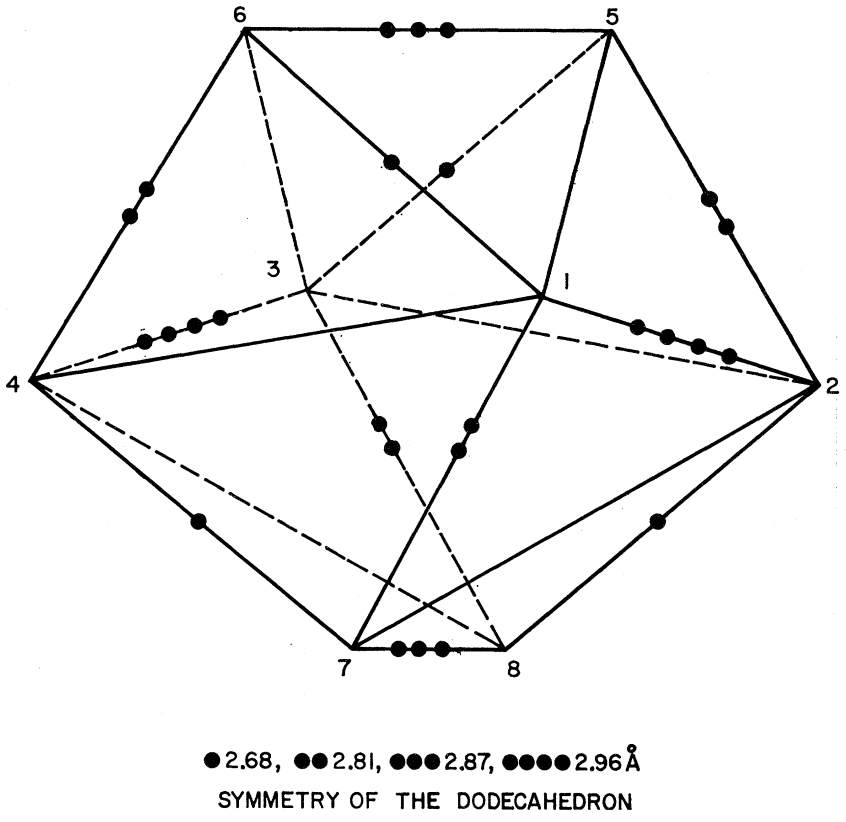

FIG. 6. Coordination dodecahedron of oxygen ions about the holmium ion (after Ref. 18).

determined are tabulated in Table VI. Since a great deal of information can be obtained from spectra of Ho in YIG, we have been able to determine all the ten exchange parameters. The energy levels of $^5I_8$ and $^5I_7$ for the four inequivalent sites in YIG calculated by the above determined parameters are shown as a function of θ in the $(1\bar{1}0)$ plane in Figs. 4(a) and 4(b), respectively. It should be noted in these figures that the energy levels of $^5I_8$ and $^5I_7$ are measured from the lowest levels of $^5I_7$ and $^5I_8$, respectively. Therefore, these figures can be directly compared with the observed variation of absorption and emission spectra shown in Figs. 6 and 7 in Ref. 1. Comparison shows that the observed variation of many of the energy levels with the direction of the magnetization are reproduced fairly well by taking into account the orbitally anisotropic exchange interaction. We note, however, that the calculated variation of some of the energy levels, in particular of $^5I_7$, is still small compared with the variation observed in absorption spectra.

In Fig. 5 we show the energy levels of Ho^{3+} in YIG in the absence of the external magnetic field in which the net magnetization directs along the [111] direction and thus the number of inequivalent sites is two as denoted by α and β in the figure. In this figure the observed values are also shown for the sake of comparison. It is seen from this figure that the calculated results are in fair agreement with the observed ones.

The discrepancy between theory and experiment, in particular in variation of absorption spectra with the direction of magnetization, may be due to the following reasons: First, as for the crystal-field parameters the approximation of three parameters may not be so good, and second, the crystal-field parameters for Ho^{3+} in YIG may be different from those for Ho^{3+} in YGaG. Third, effects of effective biquadratic exchange interactions have not been considered. In fact, the inclusion of a few percent of such exchange will give rise to a wide variation of energy levels of $^5I_7$ with the direction of magnetization.

Since the obtained exchange parameters are concerned with the over-all exchange interaction of the Ho^{3+} ion with all the neighboring Fe^{3+} ions, we must obtain from these parameters information on the exchange of the Ho ion with an individual Fe^{3+} ion. In doing so we assume that the Ho-Fe interaction takes place through the intermediary oxygen ions. As seen in Fig. 6,[18] the neighboring eight oxygen ions around a Ho^{3+} ion are classified into two types according to the distances between the Ho ion and the oxygen ions. [In Fig. 6 the oxygen ions 1, 2, 3, 4 are the nearest neighbors (type I) and the oxygen ions 5, 6, 7, 8 are the next-nearest neighbors (type II).] Thus we carry out the coordinate transformation of the exchange Hamiltonian

[18] S. Geller and M. A. Gilleo, J. Phys. Chem. Solids **3**, 30 (1967).

from the coordinate system referred to the x, y, z axes to that in which a new Z axis is taken along the line joining the Ho ion and the nearest neighbor or the next-nearest-neighbor oxygen ion. Such transformation matrices are given by Edmonds.[19] As a result and using the semiempirically determined exchange parameters in Table VI, we find that the Ho-Fe exchange interaction through the next-nearest-neighbor (type II) oxygen ion (32 cm^{-1}) is 15 times larger than that through the nearest-neighbor oxygen ion (type I). A similar result was recently pointed out by Levy[8] in the analysis of the anisotropic exchange splitting of Yb^{3+} in YbIG, and we have confirmed that the same result also holds for the Ho-Fe exchange in Ho-doped YIG.

It is concluded from the results obtained in the present section that orbitally anisotropic exchange plays an important role in the Ho-Fe exchange interaction and further that the Ho-Fe exchange interaction takes place primarily through the next-nearest-neighbor oxygen ions.

V. CONCLUSIONS AND DISCUSSION

In the present paper, the energy levels of a Ho^{3+} ion in YGaG have been calculated within the framework of crystal-field theory and then those for Ho^{3+} in YIG have been solved by taking into account the orbitally anisotropic exchange between the Ho^{3+} and Fe^{3+} ions in YIG in addition to the isotropic exchange. Observed peak positions in the spectra of Ho^{3+} ions in YGaG and YIG are fairly well reproduced by varying three crystal-field parameters, and all of the ten exchange parameters of the orbitally anisotropic exchange have been determined from the observed variation of spectra of Ho in YIG. The result of the analysis for YIG has confirmed the importance of orbital anisotropy in the rare-earth-ferric ion exchange interaction.

The calculation of the intensities of the crystal-field transitions of Ho^{3+} ions in YGaG shows that the intensity of the electric-quadrupole transition which is allowed between states of the same symmetry is smaller by order of 10^5 than that of the magnetic-dipole transition. Thus it is concluded that the electric-quadrupole transition does not contribute to the intensity of transitions between states of the same symmetry, the observed intensities being of the same order of magnitude as those calculated for magnetic-dipole transitions.

Analyzing the variation of the spectra of Ho^{3+} ions in YIG with the direction of the magnetization we have been able to assign spectra to the four inequivalent sites which the Ho^{3+} ions occupy in YIG. Using these assignments, it will be possible to determine the character of these transitions from polarization measurements.

ACKNOWLEDGMENTS

This work has been done in the collaboration with L. F. Johnson. It is a great pleasure to thank him for many invaluable discussions of his experiment and for a critical reading of the manuscript. We also wish to express our appreciation for very helpful discussions with C. G. B. Garrett, L. R. Walker, M. D. Sturge, J. F. Dillon, Jr., J. K. Galt, and D. L. Wood.

[19] A. R. Edmonds, *Angular Momentum in Quantum Mechanics* (Princeton U. P., Princeton, N. J., 1957), p. 5.